CHAPTER 9

GEOTECHNICAL DESIGN OF SHALLOW FOUNDATIONS

9.1 INTRODUCTION

The geotechnical design of shallow foundations requires specific computations for the following two purposes: (1) assurance that the foundation does not collapse by plunging into the soil or by rotating excessively and (2) assurance that the short-term and long-term total and differential settlement will be tolerable for the particular structure. The most frequent approach is to use the bearing-capacity equations in Chapter 7, or a similar set of equations, to compute the ultimate bearing stress q_d that will cause collapse; to apply a factor of safety to the ultimate bearing stress; to obtain the allowable soil bearing stress q_a; and to compute the short-term or long-term settlement with the value of q_a. These procedures are presented in detail in the following sections along with other features related to the design of shallow foundations.

9.2 PROBLEMS WITH SUBSIDENCE

Subsidence is the general settlement of the ground surface due principally to the extraction of water or perhaps oil. Subsidence can also result from the collapse of underground cavities (Gray and Meyers, 1970) or the vibration of deposits of sand (Brumund and Leonards, 1972). Lowering of the water table increases the vertical stress on water-bearing soil and on all lower strata. In simple terms, lowering of the water table means that vertical stress is increased by the total unit weight less the buoyant unit weight times the distance of the lowering. If the affected soil is compressible and fine-grained, the resulting settlement will be time-dependent and perhaps large.

Mexico City has been especially affected by subsidence (Zeevaert, 1980). Figure 9.1 shows a group of attendees at a conference in Mexico City standing next to a well casing whose top had originally been near the ground surface. The result of pumping water from strata below the city is graphically evident by comparing the exposed length of the casing to the 6-ft height of Dr. William R. Cox. If the water table is lowered uniformly and if the soil is uniform, subsidence could be uniform, but uniformity seldom exists. As noted earlier the Palace of Fine Arts has settled significantly but remains in heavy use. Some design guidelines may show that such a structure is intolerant of dif-

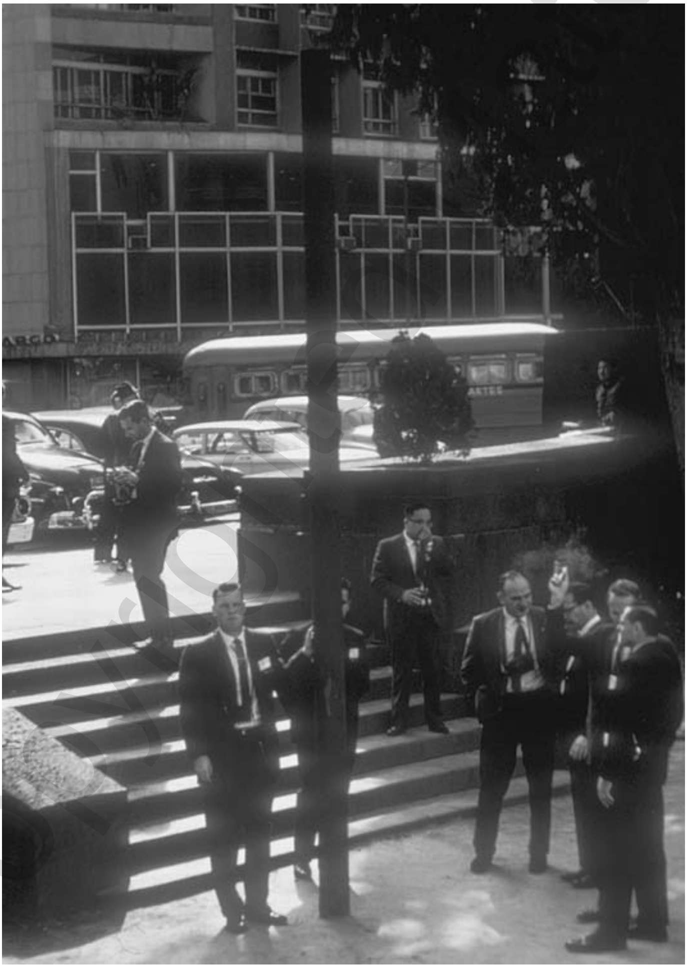

Figure 9.1 Photograph from Mexico City showing conference attendees standing next to a well casing showing subsidence over many years.

ferential settlement. The authors are reluctant to present such guidelines because of special circumstances that apply to many such structures.

Subsidence due to lowering of the water table has affected other places, including Ottawa, Canada (Bozuzuk and Penner, 1971), the Gulf Coast of Texas (Dawson, 1963), Venice (Berghinz, 1971), and London (Wilson and Grace, 1939). Surface and near-surface facilities such as roads, streets, and pipelines have been adversely affected (Zeevaert, 1980). In addition, fractures have been observed near the edges of the area of subsidence where the change in ground surface elevation was severe. Fracturing due to subsidence from the lowering of the water table is difficult and perhaps impossible to predict, but the geotechnical engineer must be aware of the chance of such occurrences.

Subsidence is a potential problem in areas of abandoned mines (Gray and Meyers, 1970) and in areas of karstic geology. Location of underground cavities emphasizes the need for a proper investigation of the soil at a site and suggests the possible use of geophysical techniques.

9.3 DESIGNS TO ACCOMMODATE CONSTRUCTION

9.3.1 Dewatering During Construction

Placing shallow foundations below the water table presents a series of challenges to the geotechnical engineer. Pumping from a sump in the excavation is frequently unacceptable because of the danger of collapse of the bottom of the excavation as a result of the lowered effective stress due to the rising water. The use of well points with good controls is usually acceptable. Furthermore, care must be taken that a nearby building is not affected by lowering the water table beneath the building.

Dr. Leonardo Zeevaert (1975) spoke of dewatering during construction of the Latino Americano Tower. Water that was removed from beneath the excavation was injected behind a sheet-pile wall to keep the water table at almost a constant elevation with respect to nearby structures. Also, records were made of a crack survey of the nearby buildings so that any new damage could be detected. No additional damage was found.

9.3.2 Dealing with Nearby Structures

Installation of foundations close to an existing structure can affect that structure. Most problems occur with the installation of deep foundations, where driving of piles or excavation for drilled shafts could cause vibrations or even the lateral movement of soil. However, an excavation with a substantial depth for a mat, for example, could create a severe problem. Extraordinary measures

must sometimes be taken, including possible underpinning of the foundations of adjacent structures.

9.4 SHALLOW FOUNDATIONS ON SAND

9.4.1 Introduction

As noted in Chapter 6, designers of footings on sand must be aware of the possible settlement due to dynamic loads. Many investigators have studied the problem, with most concern focusing on the design of compaction equipment. Brumund and Leonards (1972) performed tests in the laboratory with a tank of Ottawa sand at a relative density of 70%. A plate with a diameter of 4 in. was vibrated and a settlement of approaching 1 in. was measured. The relative density of sand deposits and all relevant properties of the sand must be considered when designing the foundations for vibrating machinery. Data provided by the machine's manufacturer must be accessed in making such a design.

The discussion in Chapter 4 indicated that sampling deposits of sand without binder below the water table is not possible without extraordinary measures, such as freezing, and in situ techniques for investigating the sand are normally required. The two principal tools for obtaining data on the characteristics of sand are the SPT and the static cone, sometimes termed the *Dutch cone.* The cone consists of a 60° hardened steel point, a projected end area of 10 cm^3, and a rate of advancement of 2 cm/sec. Data from the static cone, if obtained in the recommended manner, are reproducible because the resistance along the push rods is eliminated, the force of penetration is measured with a calibrated load cell, and the rate of penetration is standard.

The SPT has been used widely in the United States for many years and is the usual technique for determining the in situ characteristics of sand. Testing with the static cone is popular in Europe but has been slow in gaining popularity in the United States; however, many U.S. geotechnical firms can now perform the cone test.

Data from the SPT, described in Chapter 4, can vary widely from one operator to another and during the performance of a particular test. Robertson and Campanella (1988) have referenced other authors and have noted that the energy delivered to the driving rods during an SPT can vary from about 20% to 90% of the theoretical maximum, with the variation related to the number of turns of rope around the cathead, the height of fall, the type of drill rig, and the operator. They concluded that an energy ratio of 55% to 60% is the average energy level employed in the field, suggesting that SPT values have some degree of uncertainty.

In the two sections that follow, two methods are presented for obtaining the immediate settlement of shallow foundations on sand. The first is based on the static-cone test and the second is based on the SPT.

9.4.2 Immediate Settlement of Shallow Foundations on Sand

Schmertmann Method A method for estimating the settlement of shallow foundations on sand has been proposed by Schmertmann (1970) and colleagues (1978). The resistance to penetration is termed the *static-cone bearing capacity* and is given by the symbol q_c. Schmertmann noted that the values of q_c can vary widely with depth, and constant values, termed $\overline{q}_c$, are used over a particular depth. Other static-cone systems can be used for measuring the resistance of penetration if correlations are obtained with the Dutch cone.

Schmertmann's concept for the settlement of foundations on sand was to integrate the strain of the sand beneath the loaded foundation where the unit load is substantially less than the failure load. FEM studies were performed, and the results revealed that the maximum strain did not occur at the base of the foundation but at some distance below the base. Further, after a certain distance below the loaded area, the amount of strain could be considered negligible. Schmertmann and his co-workers adopted two patterns for the influence factor for strain due to rigid footings on sand, as shown in Figure 9.2, one for axisymmetrical loading and the other for plane-strain loading, as from a continuous footing. Schmertmann includes recommendations for the stiffness of the sand E_s as a function of the value of q_c or $\overline{q}_c$. The primary computation, based on experimental values of $\overline{q}_c$ and on the location and magnitude of the applied load, is modified to account for strain relief due to embedment and for time-related creep. With regard to time-related properties of sand, the phenomena related to creep or stiffening are not as evident as is the drainage of water in the settlement of soft clay, but empirical evidence is strong (Mitchell and Solymar, 1984; Mesri et al., 1990). In his original paper (1970), Schmertmann showed good to excellent agreement between computed values and values obtained from a significant number of foundations where settlement was measured.

With respect to the examples that were analyzed and the presentation that follows, it is assumed that the net load imposed by the shallow foundation does not approach the value causing a collapse. Section 9.4.3 shows the computation of the magnitude of the pressure from the shallow foundation that causes a bearing-capacity failure in the cases where settlement has been computed.

Schmertmann noted that strain ε_z at any depth z beneath a loaded area may be computed as follows:

$$\varepsilon_z = \frac{p}{E}(1 + \nu)[(1 - 2v)A + F] \tag{9.1}$$

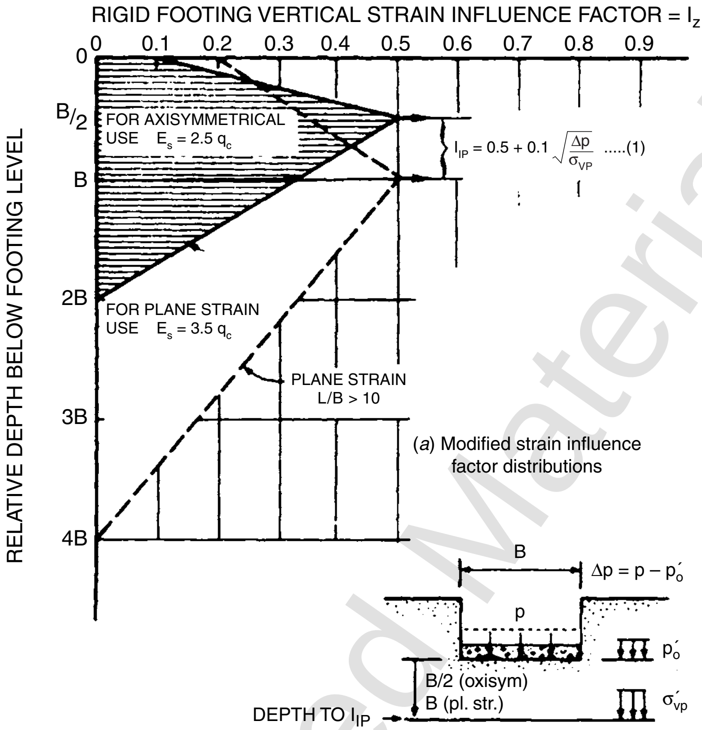

Figure 9.2 Recommended modified values for strain influence factor diagrams and matching sand moduli (from Schmertmann et al., 1978).

where

p = intensity of load on a homogeneous, isotropic, elastic half space,
E = modulus of elasticity,
ν = Poisson's ratio, and
A and F = dimensionless factors that depend on the location of the point considered.

If p and E remain constant, the vertical strain is dependent on the vertical strain factor, I_z:

$$I_z = (1 + \nu)[(1 - 2\nu)A + F] \tag{9.2}$$

The Schmertmann method for settlement is implemented by use of the following equations:

$$S_S = \int_0^{\infty} \varepsilon_z dz \cong \int_0^{f(B)} \left(\frac{I_z}{E_s}\right) dz \cong C_1 C_2 \Delta p \sum_0^{f(B)} \left(\frac{I_z}{E_s}\right) \Delta z \tag{9.3}$$

$$C_1 = 1 - 0.5\left(\frac{p_0}{\Delta p}\right) \tag{9.4}$$

$$C_2 = 1 + 0.2 \log\left(\frac{t_{yr}}{0.1}\right) \tag{9.5}$$

where

S_S = settlement according to the Schmertmann method,
$f(B)$ = $2B$ for the axisymmetric case and $4B$ for the plane-strain case (see Figure 9.2),
E_s = modulus of the sand,
C_1 = coefficient reflecting arching-compression relief,
C_2 = coefficient reflecting creep with time, and
t_{yr} = time in years.

Schmertmann and colleagues (1978) recommend that, for intermediate cases of footing shape, both diagrams in Figure 9.2 should be employed and interpolation employed for the appropriate solution.

The Schmertmann method is best demonstrated by the computation of an example that was presented in 1970 but is modified here to reflect changes presented in 1978. The footing in the example has a width of 2.60 m and a length of 23 m; therefore, the influence-factor diagram for the plane-strain case will be used. The base of the footing is 2 m below the ground surface with a unit load p of 180.4 kPa, and the overburden pressure p_0 is 31.4 kPa, yielding the net load Δp at the base of the footing of 149 kPa.

Schmertmann (1970) assumed that the cone-penetration test was performed and that values of $\overline{q}_c$ had been obtained for layers of sand of various thicknesses, starting at the base of the footing. The unit weight of the soil was assumed to be 15.7 kN/m^3 above the water table and 5.9 kN/m^3 below the water table, with the water table at the base of the footing. The diagram for plane strain may be used, but the value of I_{zp} must be increased as shown by the equation in the Figure 9.2; therefore, σ'_{vp} = (2.0)(15.7)+(2.0)(5.9) = 43.2 kN/m^3.

$$I_{zp} = 0.5 + 0.1\left(\frac{149}{43.2}\right)^{0.5} = 0.5 + 0.1(1.85) = 0.69$$

The values of I_z, shown in Figure 9.2, must be modified by increasing the value of I_{zp} from 0.5 to 0.69. The revised diagram for I_z is shown in Figure 9.3 along with assumed values of $\overline{q}_c$ from the cone test, following the pattern of values employed by Schmertmann in the original example.

The results from the computations for the revised example are shown in Table 9.1. The stratum was divided into layers, as shown in Figure 9.3, depending on values of $\overline{q}_c$, except where a layer was adjusted to fit the peak value of $\overline{q}_c$. The table extends below the footing to a depth of 4B or (4)(2.60) = 10.4 m. Eleven layers are shown in Table 9.1 with pertinent values of the relevant parameters. For a layer of a given thickness and with the corresponding value of $\overline{q}_c$, an average value of I_z was obtained by taking values at the top and bottom of each layer. The value of E_s for the plane-strain case was taken as 3.5 times $\overline{q}_c$. The values of C_1 and C_2, for a period of 5 years, were computed:

$$C_1 = 1 + 0.5\left(\frac{31.4}{149}\right) = 1.11$$

$$C_2 = 1 + 0.2 \log\left(\frac{5}{0.1}\right) = 1.34$$

The computations of settlement, layer by layer, shown in Table 9.1 yielded a total settlement of 54.1 mm, or 2.1 in. after 5 years. The immediate settle-

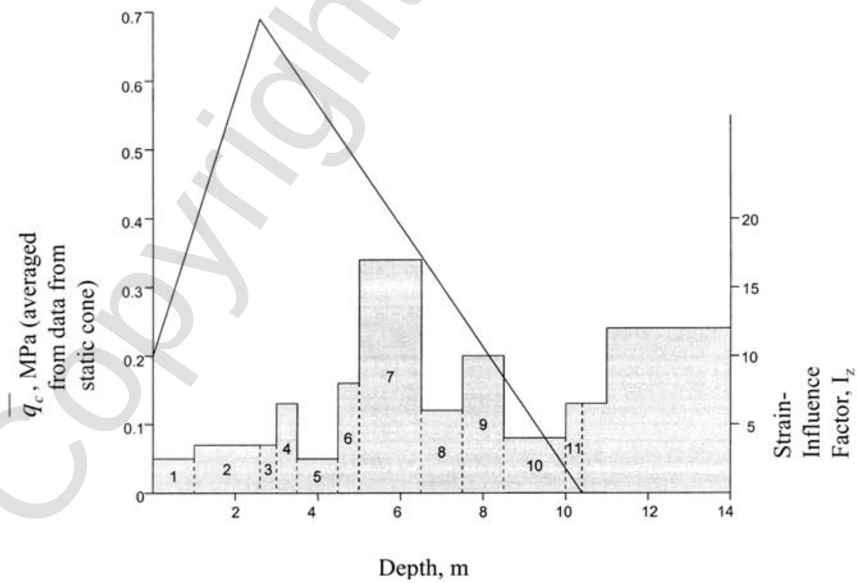

Figure 9.3 Modified strain-influence factor and assumed values of $\overline{q}_c$ from the cone test.

TABLE 9.1

Layer	ΔZ (m)	$\bar{q}_c$ (MPa)	E_s (MPa)	Z_L (m)	I_z	C_1	C_2	Δp (MPa)	Δz (m × 10^{-3})
1	1.0	2.50	8.75	0.50	0.295	1.11	1.34	0.149	7.5
2	1.6	3.50	12.25	1.80	0.540	1.11	1.34	0.149	15.6
3	0.4	3.50	12.25	2.80	0.673	1.11	1.34	0.149	4.9
4	0.5	7.00	24.50	3.25	0.633	1.11	1.34	0.149	2.9
5	1.0	3.00	10.50	4.00	0.568	1.11	1.34	0.149	12.0
6	0.5	8.50	29.75	4.75	0.500	1.11	1.34	0.149	1.9
7	1.5	17.00	59.50	5.75	0.410	1.11	1.34	0.149	2.3
8	1.0	6.00	21.00	7.00	0.300	1.11	1.34	0.149	3.2
9	1.0	10.00	35.00	8.00	0.213	1.11	1.34	0.149	1.3
10	1.5	4.00	14.00	9.25	0.103	1.11	1.34	0.149	2.4
11	0.4	6.50	22.75	10.20	0.018	1.11	1.34	0.149	0.1
									Sum = 54.1 mm

ment was computed to be (54.1)/(1.34) = 40.4 mm or 1.6 in. Schmertmann and his co-workers present a formal, step-by-step procedure for estimating the immediate and time-related settlement of shallow foundations on sand. The method is largely empirical but is founded on sound principles of mechanics and is validated by yielding reasonable comparisons with experimental values of settlement.

With regard to the magnitude of the settlement after 5 years, the geotechnical and structural engineers must decide what settlement is tolerable for the structure being designed. The informal guideline for the design of shallow foundations on sand is that settlement will control the allowable load. Frequently, a settlement of 1 in. (25.4 mm) is selected as the allowable settlement. The authors believe that the allowable settlement and the factor of safety to prevent a bearing-capacity collapse are matters to be considered for each structure, except as dictated by building codes.

An example of the bearing capacity of a shallow foundation on sand is presented in Section 9.4.3.

Peck, Hanson, and Thornburn Method The following equations present a method based on use of the SPT (Peck et al., 1974; Dunn et al., 1980). As noted, appropriate modifications are included to account for the position of water table and overburden pressure.

$$q_a = C_w(0.41)N_{SPT}S \tag{9.6}$$

$$C_w = 0.5 + 0.5\,\frac{D_w}{D_f + B} \tag{9.7}$$

where

q_a = net bearing pressure (kPa) causing a settlement S in millimeters,
C_w = term to adjust for the position of the water table,
N_{SPT} = corrected blow count from the SPT,
D_w = depth to water table from ground surface,
D_f = depth of overburden, and
B = width of footing (D_w, D_f, and B are in consistent units).

The authors included Figure 9.4 to correct N_{SPT} to account for pressure from the overburden, σ'_0 (the dependence on units should be noted).

The example of a footing on sand is shown in Figure 9.5. The footing is 3 ft by 3 ft^2 and placed 1.2 m below the ground surface. The unit weights of the sand above and below the water table are shown. The corrected value of N_{SPT} is given as 20. The above equations are used to find the value of q_a where the value of S is 25 mm.

$$C_w = 0.5 + 0.5\,\frac{1.2}{1.2 + 3} = 0.64$$

$$q_a = 0.64(0.41)(20)(25) = 131 \text{ kPa}$$

The bearing capacity of the footing in Figure 9.5 will be studied in the next section as a means of evaluating the answer shown above.

9.4.3 Bearing Capacity of Footings on Sand

The procedures presented in Chapter 7 may be used to compute the bearing capacity of the footing shown in Figure 9.5, where the corrected value of

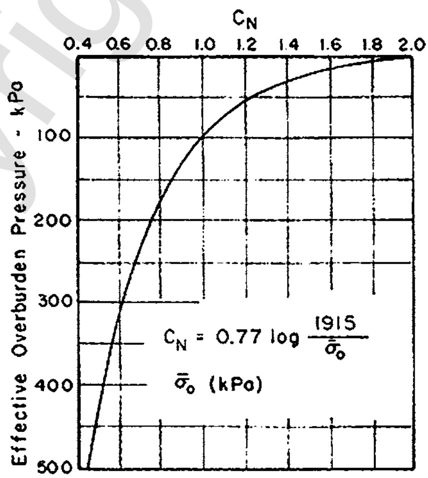

Figure 9.4 Factor used to multiply by N_{SPT} to obtain the corrected value accounting for pressure from overburden (from Peck et al., 1974).

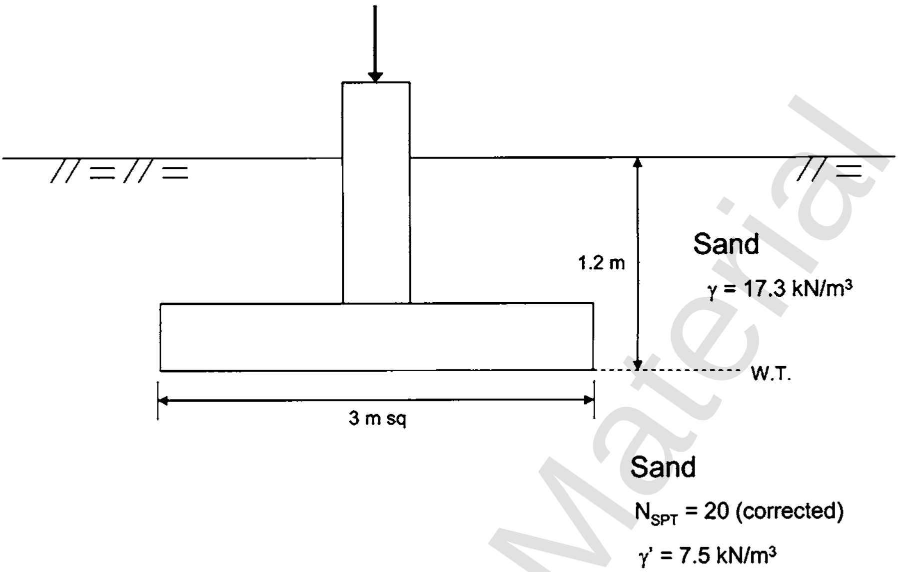

Figure 9.5 Example of a computing settlement where the value of N_{SPT} is available.

N_{SPT} is given as 20. Figure 9.6 shows a correlation between the corrected value of N_{SPT} and ϕ', where ϕ' is the friction angle from effective stress analysis. If data are available from the cone test, Figure 9.7 shows the correlation between the value of q_c from the cone test and ϕ' for uncemented quartz sand, taking the vertical effective stress into account.

For a corrected value of N_{SPT} of 20, Figure 9.6 shows the value of the friction angle ϕ' to be 33°. Table 7.1 shows the value of N_q to be 26.1 and

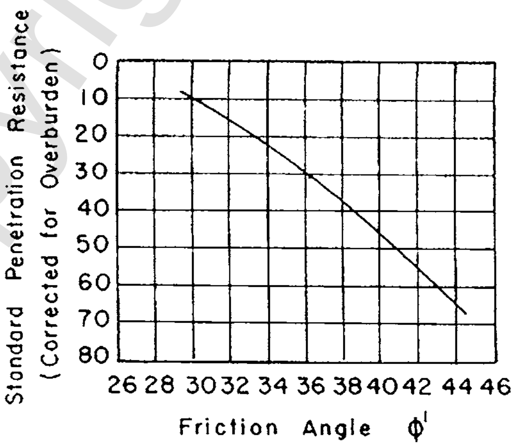

Figure 9.6 Correlation between corrected N_{SPT} and friction angle from effective stress (from Peck et al., 1974).

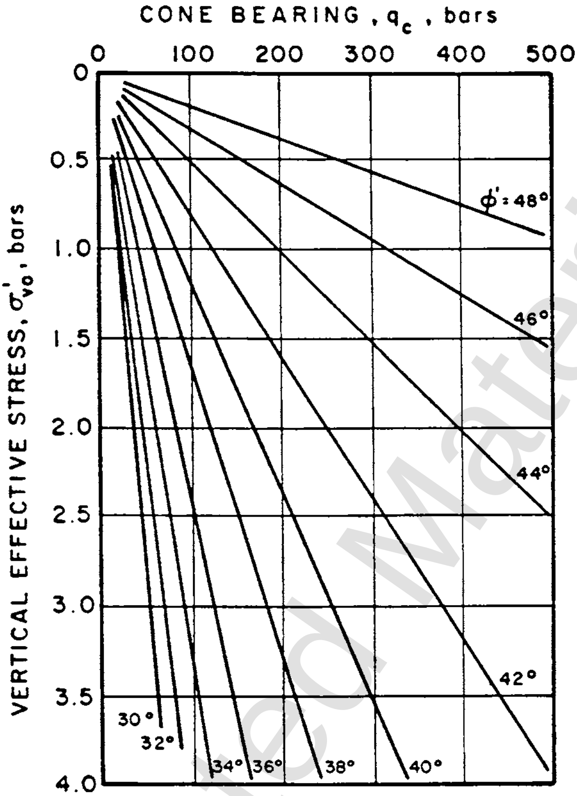

Figure 9.7 Suggested correlation between q_c from the cone test and peak friction angle Φ' for uncemented quartz sands considering vertical effective stress (from Robertson and Campanella, 1983).

the value of N_γ to be 24.4. The requisite formula is Eq. 7.7 for the case in Figure 9.5:

$$\frac{Q_d}{A} = q_d = \frac{1}{2}\,\gamma B N_\gamma s_\gamma d_\gamma + \gamma D_f N_q s_q d_q$$

where $s_\gamma = 0.6$, $s_q = 1.54$, $d_\gamma = 1$, and $d_q = 1.37$. The following values are computed:

$$q_d = \frac{1}{2}\,(7.5)(3)(24.4)(0.6)(1) + (17.3)(1.2)(26.1)(1.54)(1.37)$$

$$= 165 + 1143 = 1308 \text{ kPa}$$

If a factor of safety of 3 is employed, the value of q_a is 436 kPa. Employing the correlation shown in the previous section, the settlement for a q_a of 436 kPa would be 83 mm, a value that is too large for most structures.

This brief exercise shows that settlement will control the design of many shallow foundations on sand. However, the authors recommend that each case be considered in detail and that the decision on the value of q_a be reserved until all factors are considered.

If the cone test had been performed for uncemented quartz sand, the value of ϕ' could have been obtained from Figure 9.7. The bearing capacity q_d could have been computed by using Eq. 7.7, as shown above.

9.4.4 Design of Rafts on Sand

The procedures for computation of bearing capacity and settlement shown earlier may be extended to the design of a raft supported by sand. The principal problems facing the geotechnical engineer are (1) characterizing the soil below the raft and (2) selecting the properties to be used in the design. The geotechnical engineer will evaluate all of the available data gathered from field trips, geologic studies, and soil borings. The depth of the relevant soil beneath the footing may be selected by the following rule of thumb: use the net load at the base of the raft, use the theory of stress distribution with depth (Chapter 7), and find the depth where the stress increase under the area of heaviest load is equal to 10% or less of the net load.

Use of the rule of thumb will normally result in a depth encompassing various kinds of soil. With specific regard to a raft on sand, the properties of the sand may vary widely, perhaps as shown by the value of q_c in Figure 9.4. For the computation of settlement the sand may be considered layer by layer, but for bearing capacity, the engineer must select parameters that reflect the overall behavior of the stratum of sand. Modifying the equations for bearing capacity is not feasible, and no rule of thumb exists; instead, the engineer uses judgment, taking into account properties of the sand in the zones of maximum stress and adopting conservative values of soil properties.

9.5 SHALLOW FOUNDATIONS ON CLAY

9.5.1 Settlement from Consolidation

The procedure for predicting settlement of a shallow foundation on saturated clay was presented in Chapter 7. The theories for total settlement and for time rate of settlement are one-dimensional; that is, the flow of water from the soil is vertical, with no lateral flow or lateral strain. The theories are undoubtedly deficient for a number of reasons. Some of the deficiencies are as follows: excess porewater pressure can be dissipated by the lateral flow of

water; the stratum of clay will likely have a degree of nonuniformity, and average values must be used in the analyses; the stiffness of a structure will affect the distribution of stress and the differential settlement; and settlement can be shown to depend to some extent on the value of the pore-pressure coefficient A (Skempton and Bjerrum, 1957). In spite of the limitations noted above, the equations for total settlement and time rate of settlement of shallow foundations on saturated clay can be used with some confidence.

Skempton and Bjerrum (1957) include data on the final settlement of four structures on normally consolidated clay where settlement was significant and where the computed settlement can be compared with the observed settlement (Table 9.2). The data are undoubtedly for the portion of the structure where the settlement was largest. The computed settlement includes an estimate of the initial settlement, as discussed in the following section.

The data in Figure 9.8 are remarkable where the time rate of settlement is shown for three of the structures listed in Table 9.2 and where measurements were made over many years. Excellent agreement is indicated between observed and computed settlements over much of the life of each structure.

The procedures presented in Chapter 7 for the computations of total settlement and time rate of settlement can be used with confidence in many instances. Limitations on the theory are noted above, and implementation of the procedures can be expensive and time-consuming. Foundation investigation and laboratory studies must be of high quality, and even then the geotechnical engineer is faced with difficult decisions about relevant soil properties.

The settlement due to consolidation of clay will be illustrated using Figure 7.9a. The following assumptions are made with regard to depths and soil properties: the top of the clay layer is at 8 ft below the bottom of the footings, the clay layer has a thickness of 4 ft, the footings are embedded 2 ft into the upper sand, the upper 2 ft of the sand are saturated by capillarity, the water table is at the base of the footings, the total unit weight of the sand below the water table is 120 lb/ft^3, and the total unit weight of the clay is 110 lb/ft^3.

The effective stress at the mid-height of the clay layer prior to construction the footing may be computed as follows:

TABLE 9.2 Comparison of Observed and Computed Settlement for Four Structures

Structure	Observed Settlement (in.)	Computed Settlement (in.)
Oil tank, Isle of Grain	21	21.5
Masonic Temple, Chicago	10	12
Monadnock Block, Chicago	22	22
Auditorium tower, Chicago	24	28.5

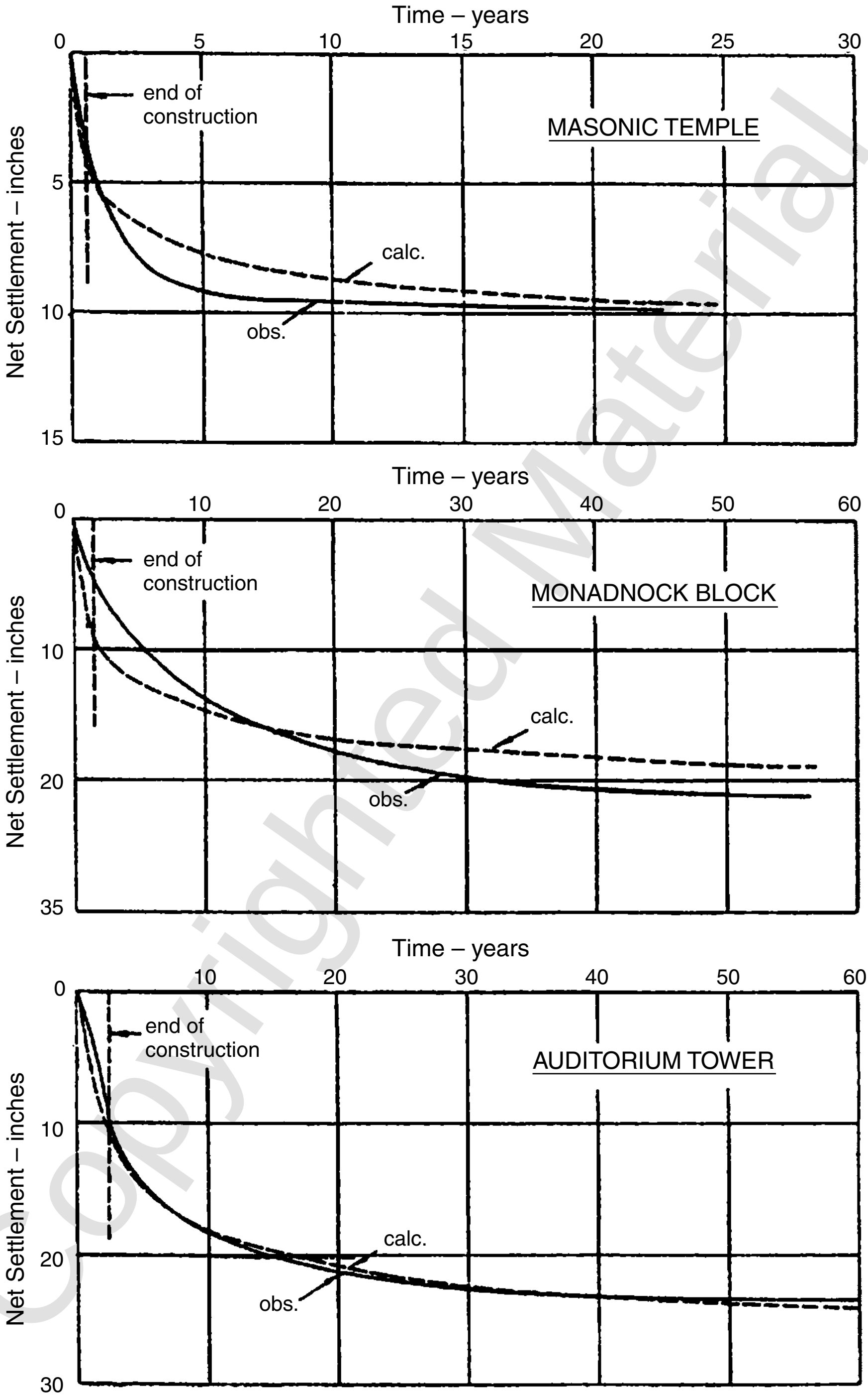

Figure 9.8 Observed and calculated settlement of buildings on Chicago clay (from Skemptom and Bjerrum, 1957).

$$\sigma'_0 = (2)(120) + (8)(120 - 62.4) + (2)(110 - 62.4) = 796 \text{ lb/ft}^2$$
$$= 0.796 \text{ k/ft}^2$$

Figure 7.12 shows that the value of σ_v was 0.580 k/ft^2 at the top of the clay layer due to the imposition of the footing loads. A similar exercise used the Newmark chart, and the value of σ_v at the bottom of the clay layer was 0.423 k/ft^2. The value of σ_v at the mid-height of the clay layer was 0.502 k/ft^2.

It is assumed that consolidation tests have been performed for the clay in the layer between the sand strata. The clay was found to be normally consolidated, and the following values were obtained: $e_0 = 0.7$, $c_c = 0.36$, and $c_r = 0.04$ ft^2/day.

From Eq. 7.36,

$$S = \frac{4}{1 + 0.7}\left[0.36 \log \frac{0.796 + 0.502}{0.796}\right] = 0.286 \text{ ft}$$

Referring to Figure 7.14, data can be obtained for preparing a table showing settlement as a function of time, as shown below. The time for a specific amount of settlement to occur may be obtained from Eq. 7.44, as shown for time for 50% of the settlement to occur.

$$T_v = \frac{c_v}{H^2}t \qquad 0.197 = \frac{0.04 \text{ ft}^2/\text{day}}{4 \text{ ft}^2}t \qquad t = 19.7 \text{ days}$$

U, %	T_v	S, ft	t, days
11	0.01	0.032	1.0
20	0.03	0.057	3.0
30	0.066	0.086	6.6
40	0.12	0.114	12.0
50	0.197	0.143	19.7
60	0.28	0.172	28.0
70	0.38	0.200	38.0
80	0.48	0.229	48.0
90	0.85	0.243	85.0
100		0.289	Infinite

Information such as that in the table above can be of great value to the engineer and other professionals in planning the design of a structure of saturated clay.

9.5.2 Immediate Settlement of Shallow Foundations on Clay

Skempton (1951) developed an equation using of some approximations of the theory of elasticity and showed the application of the methods to the imme-

diate settlement of shallow foundations. The theory of elasticity yields the following expression for the mean settlement ρ of a foundation of width B on the surface of a semi-infinite solid:

$$\rho = qBI_\rho \frac{1 - \nu^2}{E} \tag{9.8}$$

where

q = bearing pressure on the foundation,
I_p = influence value, depending on the shape and rigidity of the foundation,
ν = Poisson's ratio of the soil, and
E = modulus of elasticity of the soil.

The above equation may be rewritten in the following convenient form:

$$\frac{\rho}{B} = \frac{q}{q_d}\frac{q_d}{s_u} I_\rho \frac{1 - \nu^2}{E/s_u} \tag{9.9}$$

where

q_d = ultimate bearing capacity, ν for undrained condition of clay = ½,
I_ρ = $\pi/4$ for a rigid circular footing on the surface of the clay, and
q_d/s_u = 6.8 for the circular footing on the surface of clay as found by Skempton, where s_u is the undrained shear strength of the clay.

Making the substitutions, the following equation was obtained for a circular footing on the surface of saturated clay:

$$\frac{\rho_1}{B} = \frac{4}{E/s_u}\frac{q}{q_d} \tag{9.10}$$

Skempton noted that for footings at some depth below the ground surface, the influence value of I_ρ decreases but the bearing capacity factor N_c increases; therefore, to a first approximation, the value of $I_\rho N_c$ is constant, and Eq, (9.10) applies to all circular footings. In the axial compression test for undrained specimens of clay, the axial strain for the deviator stress of $(\sigma_1 - \sigma_3)$ is given by the following expression:

$$\varepsilon = \frac{(\sigma_1 - \sigma_3)}{E} \tag{9.11}$$

where E is the secant Young's modulus at the stress $(\sigma_1 - \sigma_3)$. The above equation may be written more conveniently as follows:

$$\varepsilon = \frac{\sigma_1 - \sigma_3}{(\sigma_1 - \sigma_3)_t} \frac{(\sigma_1 - \sigma_3)_t}{s_u} \frac{1}{E/s_u} \tag{9.12}$$

But in saturated clay with no change in water content under the applied stress, $\dfrac{(\sigma_1 - \sigma_3)_t}{s_u} = 2.0$; thus, the following equation may be written:

$$\varepsilon = \frac{2}{E/s_u} \frac{(\sigma_1 - \sigma_3)}{(\sigma_1 - \sigma_3)_t} \tag{9.13}$$

Comparing Eq. 9.10 with Eq. 9.13 shows that, for the same ratio of applied stress to ultimate stress, the strain in the loading test is related to that in the compression test by the following equation:

$$\frac{\rho_1}{B} = 2\varepsilon \tag{9.14}$$

The equation states that the settlement of a circular footing resting on the surface of a stratum of saturated clay can be found from the stress-strain curve of the clay. Skempton performed some tests with remolded London clay and found that Eq. 9.14 could be used to predict the results of the footing tests except for high values of $\dfrac{q}{q_d}$. He further noted that the values of I_ρ increased from 0.73 for a circle to 1.26 for a footing with a ratio of length to width of 10:1, while the bearing capacity factor N_c decreased from 6.2 to 5.3 for the same range of dimensions. Skempton concluded that the proposed formulation could be used with a degree of approximation of $\pm 20\%$ for any shape of footing at any depth.

9.5.3 Design of Shallow Foundations on Clay

The equations presented in Chapter 7 for computing the bearing capacity for footings of a variety of shapes, depths below ground surface, at some slope with the ground surface and in sloping soil, may be used in design. The proposal by Skempton (1951) shown above may be used for computing the immediate settlement of a shallow foundation. The applicability of the Skempton procedure will be demonstrated by analyzing experiments performed by O'Neill (1970).

O'Neill placed instruments along the length of four drilled shafts to measure the magnitude of axial load in the shafts during the performance of axial-load tests. The downward movement along each of the shafts was found by subtracting computed values of the shortening of points along the shafts from

the observed movement at the top of the shafts. The instrumentation with interpretation allowed load-settlement curves to be produced for each of the four tests.

Beaumont clay was deposited by the alluvial process in the first Wisconsin Ice Age and is somewhat heterogeneous, with inclusions of sand and silt. The liquid limit is around 70 and the plastic limit is around 20, although wide variations in both indices are common. The formation was preconsolidated by desiccation, with the indicated preconsolidation pressure at about 4 tons/ft^2. Numerous cycles of wetting and drying produced a network of randomly oriented and closely spaced fissures. The fissures led to considerable variations in measured shear strength, as indicated by the shear-strength profile shown in Figure 9.9. Confining pressure in the performance of the tests was equal to the overburden pressure. The scatter in the test results is not unusual and indicates practical problems in sampling and testing of many overconsolidated clays. The solid line in the figure was used in interpreting the results of testing of the foundation.

A stress-strain curve is shown in Figure 9.10 for the upper stratum at O'Neill's site. The shear strength was the average of two diameters below the base of each of the shafts. Significant data for the four test shafts are shown in Table 9.3. Computed values of the bearing capacity factor for three of the tests are very close to the Hansen value of 9.0. The overburden pressure and

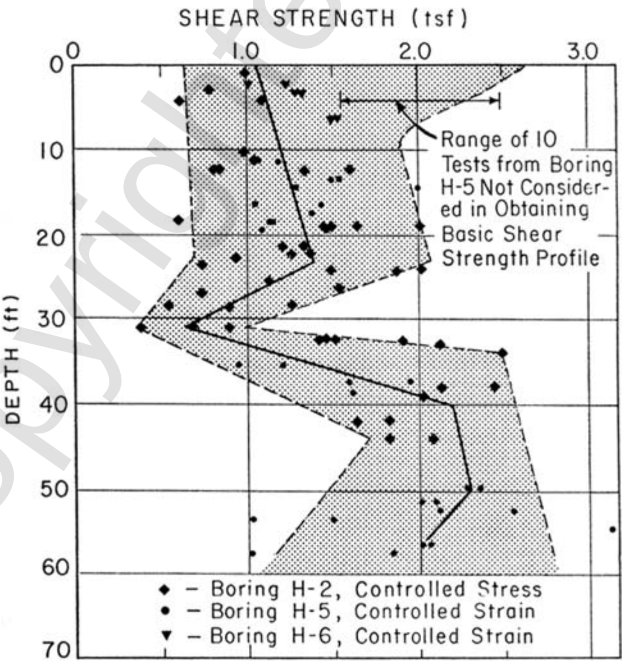

Figure 9.9 Shear strength profile from triaxial testing (from O'Neill, 1970).

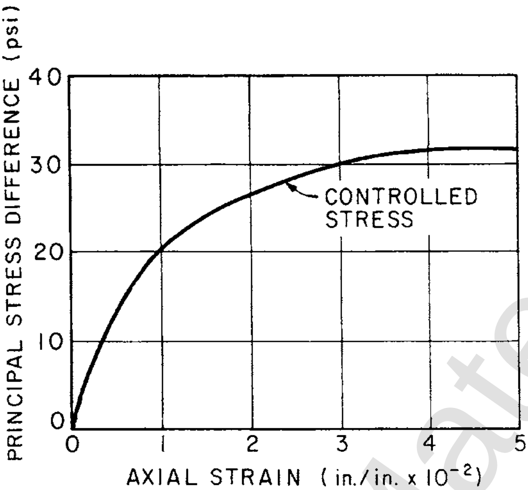

Figure 9.10 Stress-strain curves for beaumont clay (from O'Neill, 1970).

the pressure from the weight of the concrete in the drilled shaft were assumed to be equal in computing the bearing capacity.

Load-settlement curves from the experiments performed by O'Neill are plotted in Figures 9.11 through 9.14. The stress-strain curve in Figure 9.10 was used in making the Skempton computations. The lack of much better agreement between the measured and computed values is not surprising in view of the nature of the soil at the test site. The presence of randomly oriented and closely spaced fissures means that the soil in the triaxial tests was less stiff than the soil at the base of the test shafts during the testing.

As shown in Figures 9.11 to 9.14, the values for pile settlement are indicated for a factor of safety of 3 based on the data from the stress-strain curves. Assuming that the data from load tests were not available, the stress-strain curves yielded an average settlement value of 0.24 in. for the shafts with a base diameter of 30 in. and 0.27 in. for the shaft with a base diameter of 90 in. The numbers should not have caused the designer much concern, even

TABLE 9.3 Values for Each Shaft Tested by O'Neill

Shaft Designation	Penetration (ft)	Diameter of Base (in.)	Avg. S_u at 2D Below Base (tsf)	Ultimate Load on Base (tons)	Computed Value of N_c
S1	23	30	1.16	52	8.91
S2	23	90	1.16	445	8.68
S3	24	30	1.05	47	9.12
S4	45	30	2.28	142	12.68

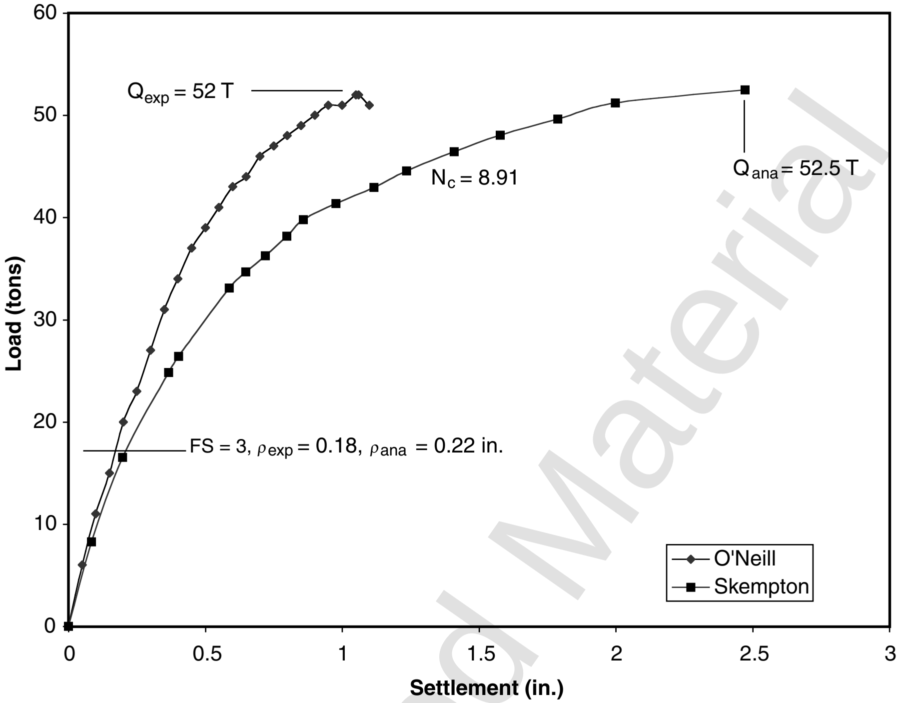

Figure 9.11 Load-settlement curves for test shaft S1.

though the corresponding numbers from the load tests were 0.18 in., 0.05 in., and 0.09 in. (shafts 1, 3 and 4), average of 0.11 in. and 0.21 in.

9.5.4 Design of Rafts

The comments on the design of rafts on sand apply as well to the design of rafts on clay. The equations for bearing capacity and settlement of shallow foundations presented in Chapter 7 may be used. Emphasis is placed on a soil investigation and a laboratory study of high quality. The engineer must exercise extra care in selecting parameters for use in design. If differential settlement is revealed to be a problem, the geotechnical engineer may work closely with the architect and the structural engineer in placing and sizing the shallow foundations to achieve an optimal solution.

9.6 SHALLOW FOUNDATIONS SUBJECTED TO VIBRATORY LOADING

The response of foundations under dynamic loads is significantly different from that under static loads. The analysis and design of foundations subjected

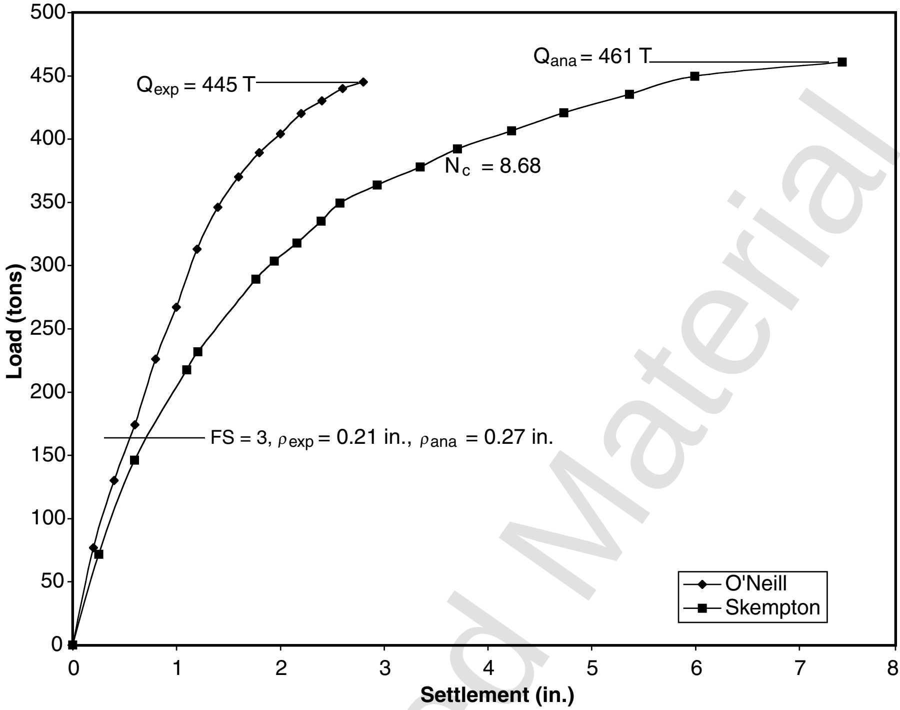

Figure 9.12 Load-settlement curves for test shaft S2.

to machine vibration or impact from earthquake is a difficult problem because of the complex interaction between the structural system and supporting soil/rock stratum. The proper solution of the problem requires an accurate prediction of the foundation response to these loads. A complete and rigorous analysis must account for the following: the three-dimensional nature of the problem, material and radiation damping of the soil, variation of soil properties with depth, embedment effects, and interaction effects between multiple foundations through the soil. In the last 30 years a number of solutions have been developed for design of machine foundations. Extensive reviews of these developments were presented by Richart et al (1970), Lysmer (1978), Roessett (1980), Gazetas (1983, 1991), and Novak (1987). These are beyond the current scope of this book.

The topic is discussed here to emphasize the fact that the vibration of sand can cause densification of the sand with consequent settlement of the foundation. Therefore, the geotechnical engineer must consider the relative density of the sand at the site. If it is close to unity, vibration is likely not to be a problem. Otherwise, settlement will occur and provisions must be made to deal with it.

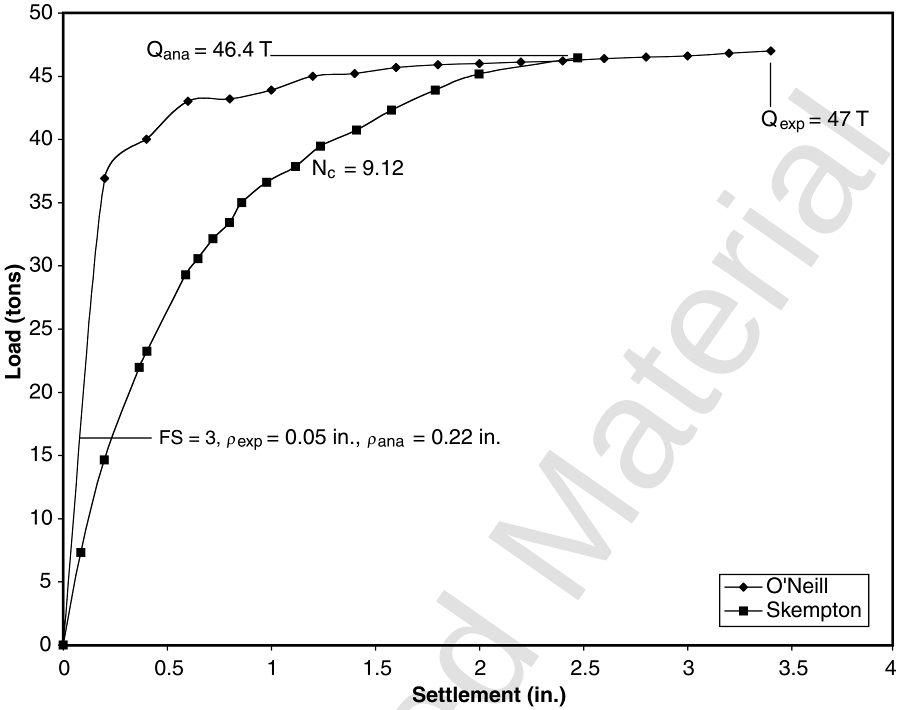

Figure 9.13 Load-settlement curves for test shaft S3.

Two procedures may be considered: (1) the use of deep foundations driven into stable soil with respect to vibration and (2) the use of soil-improvement methods to make the sand resistant to vibration.

9.7 DESIGNS IN SPECIAL CIRCUMSTANCES

9.7.1 Freezing Weather

Frost Action The depth of freezing of the soil in regions of the United States and areas to the south of Canada is shown in Figure 9.15. Ice lenses may form if the frozen surface soils include significant moisture, and the expansion due to the ice could cause some heave of the foundation. Engineers in cold climates must consult local building codes on the required depth of shallow foundations, taking into account the nature of the soils. A particular problem occurs if the soil at and above the water table consists of silt and fine sand, as shown in Figure 9.16.

The capillary rise in the granular soil between the water table and the shallow foundation allows water to accumulate in quantities, creating ice

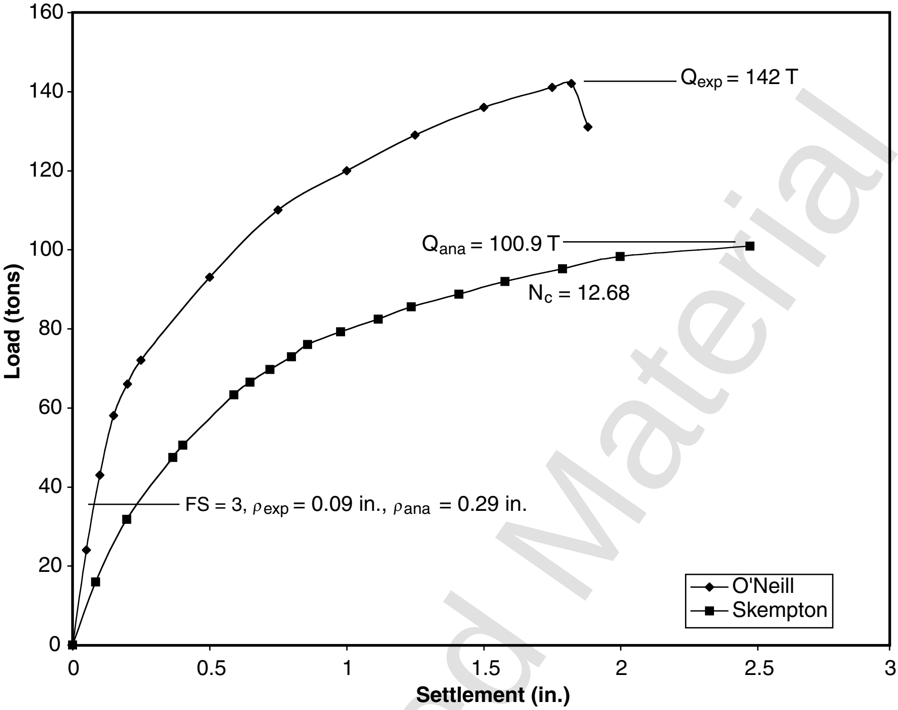

Figure 9.14 Load-settlement curves for test shaft S4.

lenses. With time, more water rises and additional ice lenses are formed. On some occasions, a large quantity of ice can collect in a restricted area. The increased thickness of the ice causes a heave of the shallow foundation, as shown in Figure 9.16. When warm weather occurs the ice in the soil melts, leaving the soil with high water content and a low value of bearing capacity. The conditions shown in Figure 9.15 can lead to failures of roadway pavement that can be dangerous to vehicular traffic. A remedy to the problem illustrated in Figure 9.16 is to place a layer of coarse granular soil in the zone of capillary rise to prevent the upper flow of capillary water.

In northern climates, the soil may remain permanently frozen, a condition termed *permafrost.* The construction of light structures and other facilities in such regions is aimed at preventing the thawing of the permafrost. Structures are supported on posts or short piles so that air circulation beneath the structure and above the frozen soil is allowed to continue.

Placing Concrete Freezing weather increases the cost of construction because the concrete must be protected. The protection against freezing must last until the concrete "takes a set" or hardens so that free water is not present. In some climates where freezing weather continues for many months, foun-

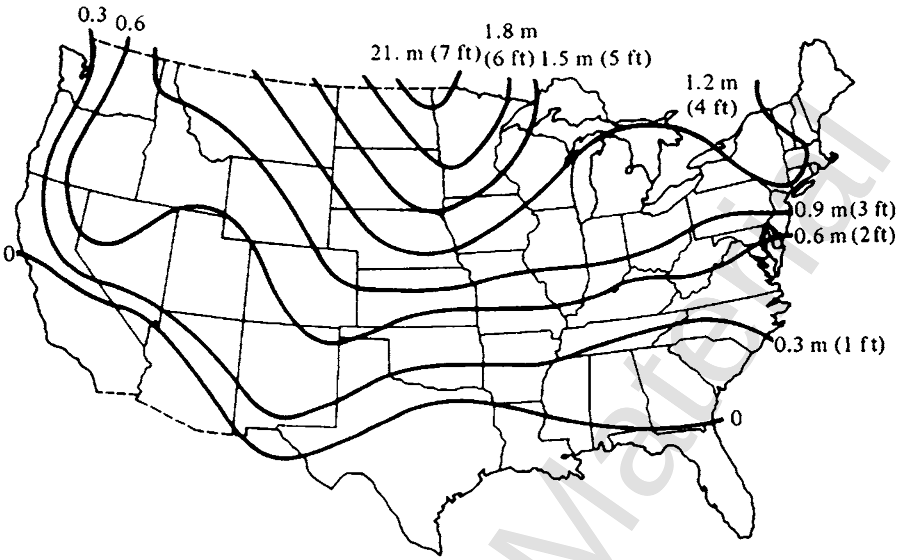

Figure 9.15 Maximum anticipated depths of freezing as inferred from city building codes. Actual depths may vary considerably, depending on cover, soil, soil moisture, topography, and weather (from Spangler and Handy, 1982).

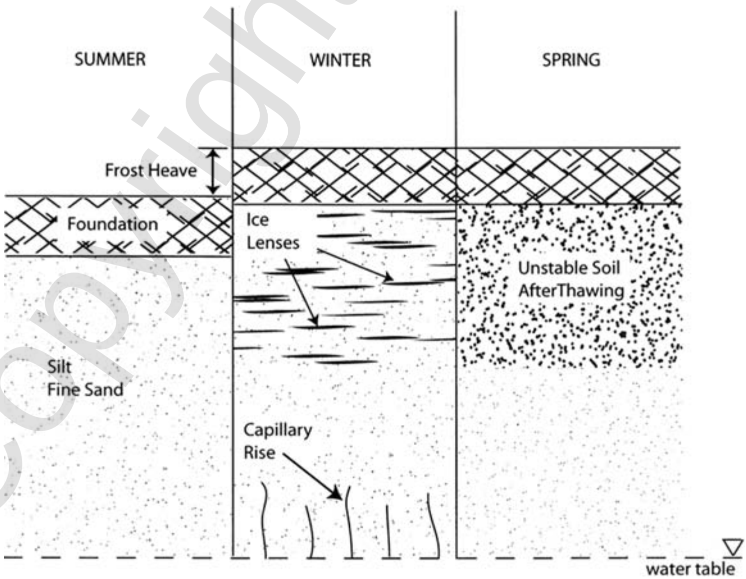

Figure 9.16 Sketches of frost action.

dation elements have been prefabricated in workshops and placed in prepared areas at the job site. Short-term settlement is more likely to occur with prefabricated foundations because the contact between the soil and the foundation is less than perfect.

9.7.2 Design of Shallow Foundations on Collapsible Soil

Collapsible soils were described briefly in Chapter 2. Such soils consist of thick strata of windblown fine grains, deposited over long periods of time, and reinforced by remains of vegetation or by cementation. The soil will remain stable under moderate loads as determined by the appropriate testing procedures; however, on becoming saturated, the soils will collapse. Preventing a rising water table or saturation from precipitation is essential. Therefore, if drainage can be assured or a rising water table can be prevented, shallow foundations can be installed and will remain stable. If saturation of the collapsible soil is judged to be possible, some form of deep foundation will be necessary.

9.7.3 Design of Shallow Foundations on Expansive Clay

Expansive clay is an extremely troublesome foundation material and exists widely in the United States, as shown in Figure 9.17. Chapters 2 and 6 present some of the factors related to expansive clay. Owners of homes and small businesses must pay a premium for building or repairing the foundation. Otherwise, they will be left with a substandard and unsightly structure.

The soil at a particular site may appear to be firm and substantial, and potential foundation problems may not be evident. Unfortunately, the local building codes in many cities may not address the requirements for identifying expansive clay and then specifying appropriate procedures for constructing a foundation if expansive clay is present. Furthermore, years may pass before the damage from an improper foundation becomes evident.

Expansive clay is readily seen if a site is visited during dry weather. Cracks in the surface soil are visible and may extend several feet below ground surface. Geotechnical investigations to identify the problem may involve several kinds of laboratory tests. These tests include liquid limit, plastic limit, shrinkage limit, swelling pressure under confinement, free-swell test, and identification of clay minerals. Tables 9.4 and 9.5 give recommendations for indicating the swelling potential of clay on the basis of laboratory tests.

The value of the plasticity index is used by many engineers to evaluate the character of a clay soil. Tables 9.4 and 9.5 suggest that a plasticity index of 15 or less means that the clay is expected to swell very little, if at all.

If a clay soil is judged to be expansive, the thickness of the zone is considered. If it is shallow, the troublesome soil may be removed. Alternatively, the expansive clay may be treated with chemicals such as lime. The lime must be mixed with the soil by tilling, not by the injection of a slurry of lime and

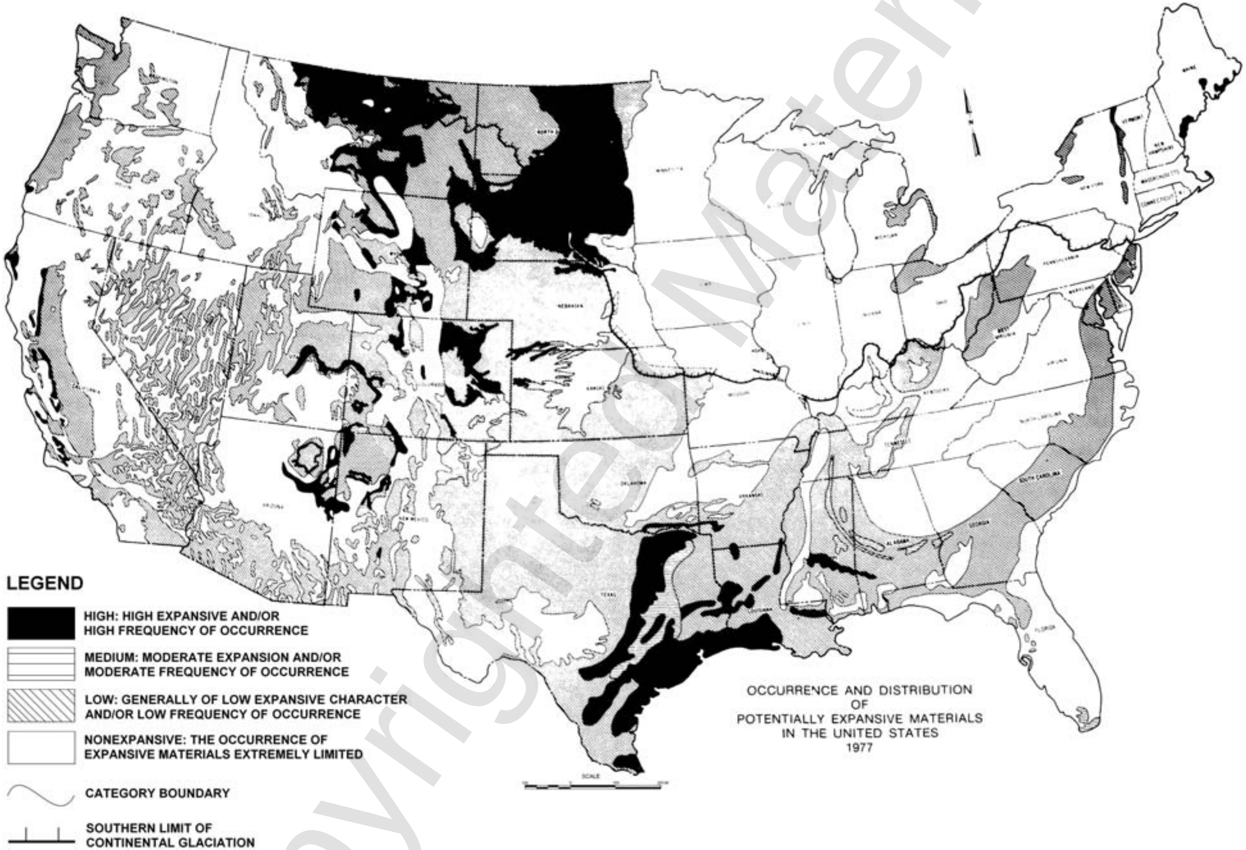

Figure 9.17 Distribution of potentially expansive soils in the United States (from Nelson and Miller, 1992).

TABLE 9.4 Swelling Potential from Laboratory Tests

Percentage of Sample Less Than 1 μm	Plasticity Index	Shrinkage Limit	Percentage of Volume Expansion from Dry to Saturation
>28	>35	<11	>30
20–31	25–41	7–12	20–30
13–23	15–28	10–16	10–20
<15	<18	>15	<10

Source: Holtz and Gibbs (1954).

water. The permeability of clay is so low that the slurry will not readily penetrate it.

If the stratum of clay is so thick that it cannot be removed or treated, then the engineer usually considers the use of a stiffened slab on grade, such as the BRAB slab (Building Research Advisory Board, 1968). The site is graded with deepened sections at relatively close spacing where reinforcing steel is placed to form beams into the foundation. The depth of the beams and the spacing depend on the judgment about shrinkage potential. The purpose of the beams is to make the slab so stiff that differential settlement is minimal. Over time, moisture will collect under the center of the slab because of restricted evaporation, but the edges of the slab will respond to changes in weather. Some homeowners have used plantings or other means to prevent shrinkage of the soil around a stiffened slab.

In some cases, a founding stratum may occur below the expansive clay. Drilled shafts can be installed with bells and designed to sustain the uplift from the expanding clay. If drilled shafts are used, a beam system should be employed to provide a space above the surface of the clay to allow swelling to occur without contact with the beams and floor system. Further, the bond between the expanding clay and the shaft should be eliminated or the shaft should be heavily reinforced to sustain uplift forces.

9.7.4 Design of Shallow Foundations on Layered Soil

Rarely does the geotechnical engineer encounter a design where the founding stratum is uniform and homogeneous. The reverse is usually the case; either

TABLE 9.5 Swelling Potential from the Plasticity Index

Swelling Potential	Plasticity Index
Low	0–15
Medium	10–15
High	35–55
Very high	≥55

Source: Chen (1988).

the soil is of the same sort but with widely varying properties, or two or more layers exist in the zone beneath the foundation. Settlement may be computed with procedures that have been presented, but questions arise when selecting the bearing capacity. If the additional cost is minor, the bearing capacity may be based on the weakest stratum in the founding stratum. The second possibility is that settlement will control the design, as shown earlier in this chapter, rather than bearing capacity.

In some studies, the shapes of the failure surfaces have been modified to reflect the presence of layers with different characteristics (Meyerhof, 1978; Meyerhof and Hanna, 1974). A more favorable approach is to employ FEM, as demonstrated by the material in the following section. A number of codes are available. Such codes will continue to be important in the analytical work of engineering offices.

9.7.5 Analysis of Response of a Strip Footing by Finite Element Method

As noted in the previous section, the FEM may be used to a considerable advantage in the analysis of shallow foundations. The application to the following example is an elementary use of FEM by serves to indicate the power of the method. A strip footing with a width, B, of 120 in. is resting on the surface of a soil, Figure 9.18, with the following characteristics: E = 30,000 psi, v = 0.3, c = 10 psi, and ϕ = 20°. The unit weight of the soil was

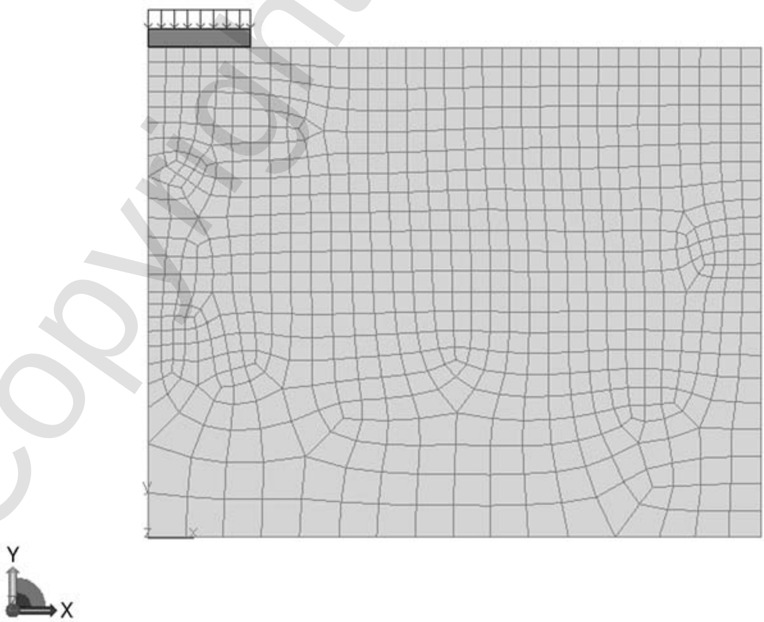

Figure 9.18 Model of a strip footing by FEM.

assumed to be 120 pcf. The Mohr-Coulomb model was used to represent the nonlinear behavior of the soil.

The result from the FEM computation, where a series of deformations of the footing was used as input, is shown in Figure 9.19. The analysis assumed a rough footing because the soil was not allowed to spread at the base of the footing. As may be seen, the unit value of the ultimate bearing capacity (q_u) of the footing was predicted as 185 psi. The Terzaghi equation for bearing capacity, Eq. 7.3, is re-written to obtain the unit value of ultimate bearing capacity and shown in Eq. 9.15.

$$q_u = \frac{1}{2}\gamma B N_\gamma + \gamma D_f N_q + c N_c \tag{9.15}$$

The footing is resting on the soil surface, so the value of D_f is 0. The properties of the soil show above were employed, along with the following values of the bearing capacity factors (see Chap 7): $N_\gamma = 3.64$, $N_c = 17.69$, and the value of q_u was computed as follows

$$q_u = \frac{1}{2}(0.0694)(120)(3.64) + (10)(17.69) = 15.2 + 176.9 = 192.1 \text{ psi.}$$

The FEM yielded a value quite close to the result from the Terzaghi equations. The methods presented herein do not allow a check to be made of the initial slope of the load-settlement curve in Fig. 9.19. The deformation field of soil in the vicinity of the strip footing generated by the FEM output is presented in Fig. 9.20 which is consistent with the theory introduced in Chapter 7.

The excellent comparison between results from the FEM for a solution of a straightforward problem indicates that the method can be applied to complex problems in bearing capacity including response to eccentric loading and behavior of shallow foundations on layered soils. However, in the solution of

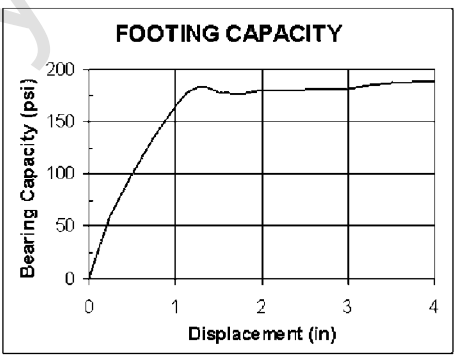

Figure 9.19 Load-settlement curve for a strip footing from analysis by FEM.

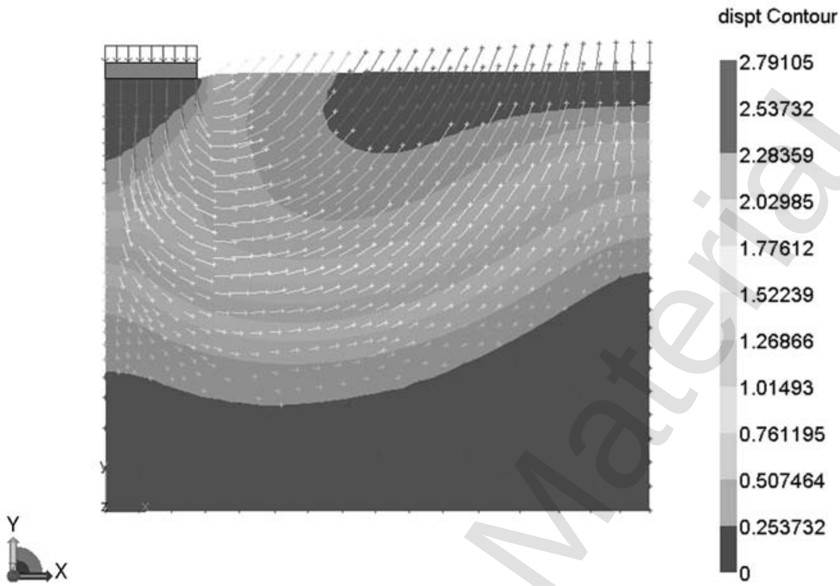

Figure 9.20 Deformation field for soil near a strip footing from analysis by FEM.

the example, the engineer faced the problem of selecting a constitutive model for the soil, the size and number of the elements, the distance to each of the boundaries, and appropriate restraint at the boundaries. Experience in using the method is valuable, but different trials by varying the parameters in the solution may be necessary. Many engineering offices are routinely employing codes for the FEM and more use is expected in the future.

PROBLEMS

P9.1. Cummings (1947) described the nature of the clay in the Valley of Mexico and showed the results of consolidation tests performed at Harvard, where the void ratios were extremely high and unusual.

The *e*-log-*p* plot in Figure 9.21 is patterned after the test results reported by Cummings. Using that plot and estimating the settlement at a location in Mexico City from the photograph in Figure 9.1, compute the amount the water table must be lowered to cause the settlement indicated. Assume the clay stratum to be 150 ft thick, the initial void ratio to be 6.60, the initial compressive stress to be 0.9 tsf, and that the clay remains saturated by capillarity as the water table is lowered. The answer may be surprising.

P9.2. The plot in Figure 9.22 shows values of q_c from the cone penetration test at a site where a footing is to be constructed. Use the Schmert-

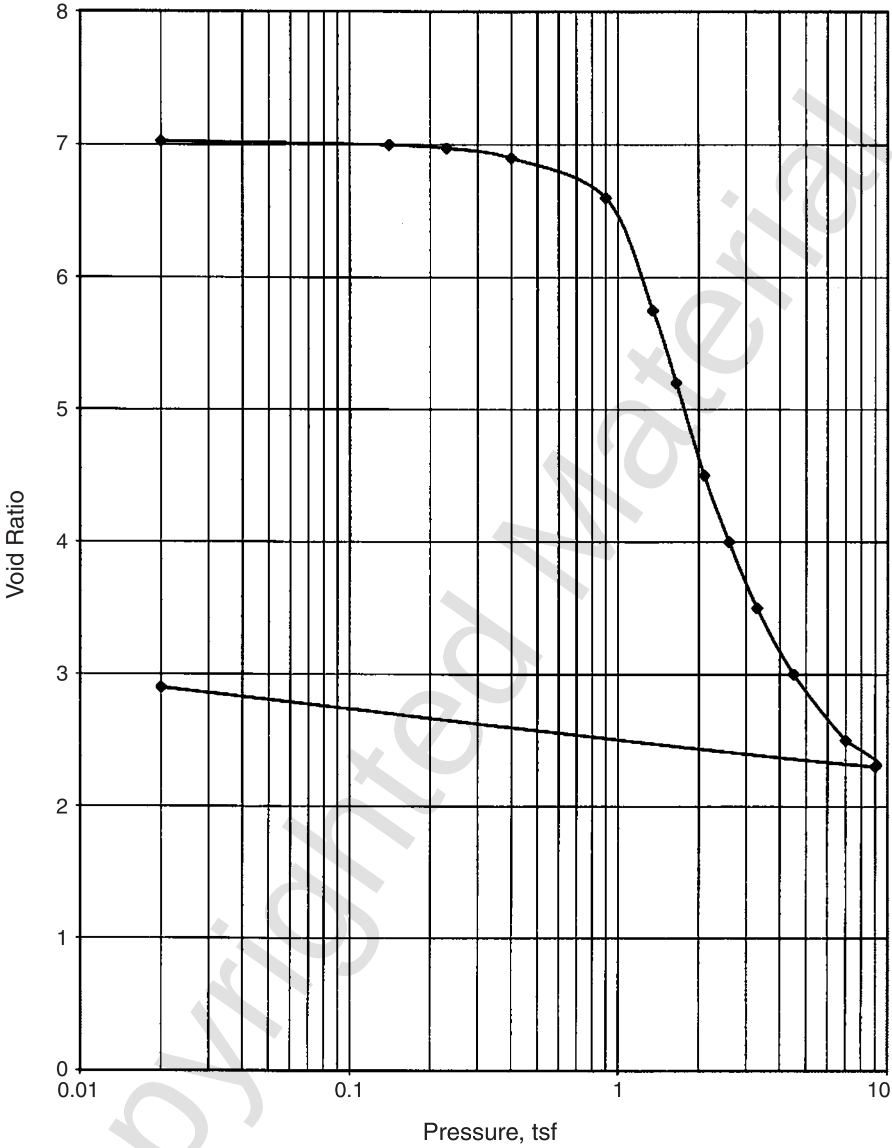

Figure 9.21 Plot of *e* versus log-*p* for soil similar to that in the Valley of Mexico.

mann method to compute the settlement of a square footing, 2 by 2 m in plan, with its base at 1 m below the ground surface. Assume that the soil is sand with an average grain size of 0.5 mm and a submerged unit weight of 9.35 kN/m^3. The load at the base of the footing is 80 kPa. Use three layers below the base of the footing in making settlement computations for 1 year and 10 years.

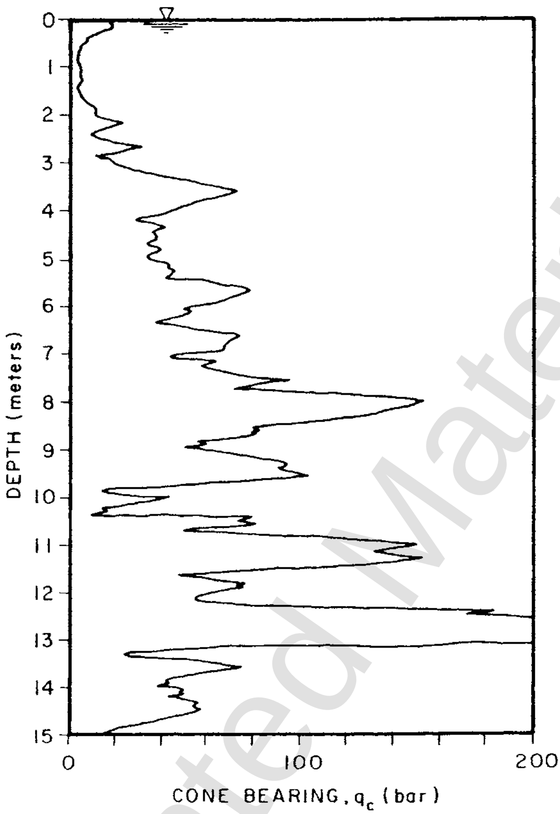

Figure 9.22 Example of the result of the cone penetration test (from Robertson and Campanella, 1988).

P9.3. Use the data from Problem P9.2 to compute the bearing capacity for the footing. Use Figure 9.23 in selecting a value of ϕ for use in bearing-capacity computations, and consider the low value q_c at the base of the footing and the significant increase with depth below the base. Assume a factor of safety of 3 and compute the value of the safe bearing capacity. Compare the safe bearing capacity with the unit load used in Problem P9.2. Discuss the allowable load or safe load you would select. (Check construction on figure and modify as necessary.)

P9.4. Estimate the settlement of a footing 10 ft^2 resting at a depth of 2 ft below the surface of a coarse sand and subjected to a total load of 400 kips. The water table is at a depth of 2 ft, and the corrected value of N_{SPT} is 30.

P9.5. Compute the unit bearing capacity in kips per square foot of the footing in Problem P9.4, assuming that the total unit weight of the sand is 122 pcf. Compute the factor of safety for the load of 400 kips.

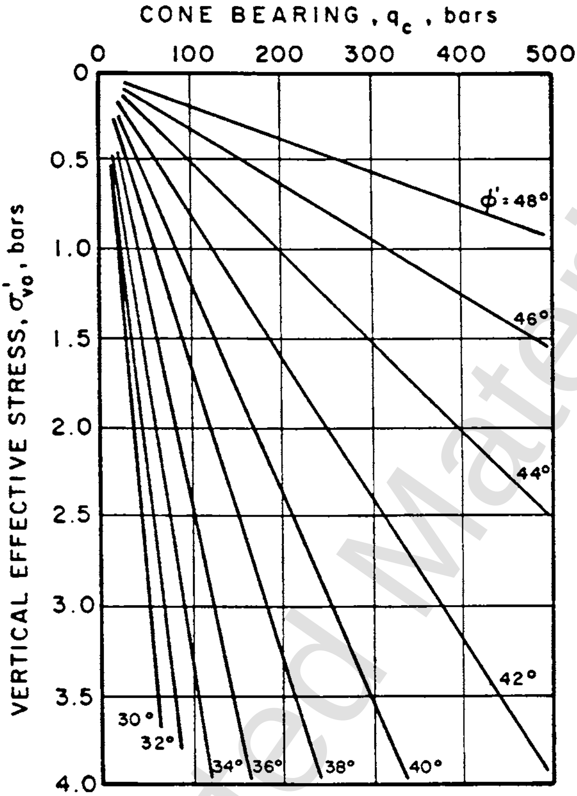

Figure 9.23 Suggested correlation between q_c from the cone test and peak friction angle Φ' for uncemented quartz sands considering vertical effective stress (from Robertson and Campanella, 1983).

P9.6. The unconfined compressive strength of a clay is 1.2 kips/ft^2, the water table is 4 ft below the ground surface, the total unit weight of the clay γ is 118 lb/ft^3, and a drilled shaft with a diameter of 4.25 ft placed at a depth of 10 ft supports a column load by end bearing only. (a) Use a factor of safety of 2.8 and compute the safe column load on the foundation. (b) An excavation near the drilled shaft removes the soil down to the water table. What is the effect on the factor of safety?

P9.7. A water tank with a height of 25 ft and a diameter of 50 ft rests on a stratum of sand with a thickness of 12 ft. A stratum of clay with a thickness of 20 ft exists below the sand, and a thin layer of gravel exists below the clay. The water table is at the surface of the clay. Plot a curve showing the stress increase in the clay as a function of depth for the center and edge of the tank. Assume the tank to be filled with water to a depth of 23 ft. Ignore the weight of the steel in the tank.

P9.8. Assume that consolidation tests were performed on the clay in Problem P9.7, that the soil is normally consolidated, and that the following values were obtained for the clay: $\gamma_{sat} = 120$ pcf; $e_0 = 1.10$; $c_c = 0.40$; $c_v = 0.025\ \mathrm{ft^2/day}$; sand, $\gamma = 125$ pcf. Compute the settlement in inches at the center and edge of the tank.

P9.9. Plot curves showing the settlement of the center of the tank as a function of time.

P9.10. Plot a curve showing the distribution of excess porewater pressure in the clay stratum for consolidation of about 50% (use $T_v = 0.2$).

P9.11. If the differential settlement of the tank is judged to be a problem, list three steps that may be taken to reduce it.